

Investigation of the Binding Properties of 3,4-Dihydroxybenzaldehyde from *Salvia miltiorrhiza* (Bunge) with Human Serum Albumin via Multi-spectroscopic and Molecular Docking Techniques

Haibo Liu,^{a,b} Jiaqian Wang,^a Yonglin He,^b Wenwen Zhang,^a Lei Lei,^a Long Chen,^a Yalan Chen,^a Jing Zhu,^{a,*} Juncai Tu,^c and Kun Li^{a,*}

To investigate the binding properties of 3,4-dihydroxybenzaldehyde with human serum albumin, as well as the structural changes of human serum albumin under a simulated physiological pH value (a pH of 7.4) and a high 3,4-dihydroxybenzaldehyde concentration, a series of techniques, *i.e.*, fluorescence, synchronous fluorescence, ultraviolet-visible absorption, Fourier-transform infrared spectroscopy, and molecular docking simulation, were employed. Steady state fluorescence showed that 3,4-dihydroxybenzaldehyde quenched the intrinsic fluorescence of human serum albumin via a static mechanism. The 3,4-dihydroxybenzaldehyde-human serum albumin complex had a strong affinity ($K_b = 10^5 \text{ M}^{-1}$) at various temperatures. It was shown that 3,4-dihydroxybenzaldehyde was bound to the IB subdomain of human serum albumin primarily via hydrogen bonding and van der Waals forces at high 3,4-dihydroxybenzaldehyde concentrations, based on the results of the thermodynamic and molecular docking. Furthermore, the fluorescence emission spectrum and Fourier-transform infrared spectroscopy results indicated that the binding distance between 3,4-dihydroxybenzaldehyde and human serum albumin was 4.42 nm. In addition, 3,4-dihydroxybenzaldehyde induced conformational changes of human serum albumin. These findings provide reasonable evidence for further understanding the distribution of 3,4-dihydroxybenzaldehyde when it spreads into human blood serum, which may be helpful in food and medicine research.

DOI: 10.15376/biores.17.2.2680-2695

Keywords: 3,4-Dihydroxybenzaldehyde; Human serum albumin; Interaction mechanism; Spectroscopy; Molecular docking

Contact information: a: Xinyang Agriculture and Forestry University, Xinyang 464000 China; b: College of Food Science, Southwest University, Chongqing 400715 China; c: Department of Wine, Food and Molecular Biosciences, Lincoln University, P. O. Box 84, Lincoln, Christchurch 7647 New Zealand;

* Corresponding author: zhujingcy@163.com; likunkm@163.com (K. Li)

INTRODUCTION

Human serum albumin (HSA) is a carrier protein that plays an important role in the transport, deposition, distribution, and transformation of all types of different exogenous and endogenous substances, including enzymes, nutrients, metal ions, fatty acids, hormones, steroids, and surfactants (Cui *et al.* 2008; Yan *et al.* 2015). It has been reported that the high-affinity binding between HSA and a drug can reduce the free concentration of the drug, which may increase or decrease the advantage in the drug efficacy (Yue *et al.*

2018). However, low-affinity binding can result in poor distribution and a shorter lifetime of the drug (Sun *et al.* 2017). Therefore, establishing a balance between the bound form and the free fraction of the drug to gain suitable therapeutic doses is very important, because only in this way can a balanced amount be sent to target tissues. Simultaneously, a balance between the appropriate stay time and the clearance of the drug should be maintained so as to decrease its toxic side effects (Caruso *et al.* 2016; Nusrat *et al.* 2018). Upon examination, additional study of the binding properties of various drugs with HSA is imperative.

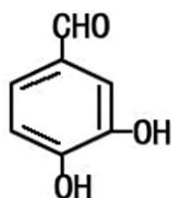


Fig. 1. The chemical structure of 3,4-dihydroxybenzaldehyde

As shown in Fig. 1, protocatechualdehyde (PCA), is an antioxidant that is present in *Salvia miltiorrhiza* (Bunge) (Li *et al.* 2016). It has been shown that PCA has many different health benefits, including anti-atherosclerosis, antioxidant properties, and anti-inflammatory and anti-cancer effects (Duan *et al.* 2019; Li *et al.* 2020). Recently, the molecular interaction of small drug molecules with HSA has attracted much attention due to the fact that the binding properties of both may influence the pharmacokinetics and toxicity of small drug molecules *in vivo* (Almutairi *et al.* 2020). The binding mode of HSA and PCA at low concentrations was studied *via* the synchronous fluorescence method (Tian *et al.* 2011). The results showed that PCA was primarily bound to HSA through electrostatic and hydrophobic interactions at a relatively low concentration area, *i.e.*, a PCA range of 0 mol/L to 27.97×10^{-7} mol/L. Several studies have explored the interaction between different proteins (such as soy protein isolate, casein, bovine serum albumin, β -lactoglobulin) and other substances with different properties (such as structure and chain length). The studies mainly have focused on the binding abilities between proteins and other substances influenced by the properties of proteins and alcohols, and processing conditions (such as pH, heat treatment and oxidation treatment). Binding of proteins to other substances causes changes in amino acid residues, which lead to changes in protein conformation, resulting in fluorescence quenching (Guo *et al.* 2020; Wang *et al.* 2021). However, the binding mode between small molecules and proteins is not static and is affected by many factors, *e.g.*, environmental conditions and competitive effects (Ni *et al.* 2011; Malhotra and Karanicolas 2017). Therefore, this stimulated the interest of the authors in terms of exploring the binding mode of HAS with a high-concentration PCA.

In this work, fluorescence, synchronous fluorescence, ultraviolet-visible absorption (UV-vis), Fourier-transform infrared (FT-IR) spectroscopy, and molecular docking simulation were used to determine the binding interaction of PCA with HSA in order to elucidate the molecular mechanism of the binding process at a high concentration of PCA. The data for the quenching mechanism, binding constants and number of binding sites, thermodynamic parameters and binding interaction force, binding distance, binding site, and HSA microenvironmental and conformational changes were obtained. This work may provide a more detailed reference for studying the binding properties of PCA with HSA *in vivo*.

EXPERIMENTAL

Materials

The PCA (CAS Number: 139-85-5, with a purity greater or equal to 98%) was bought from Chengdu Must Bio-Technology Co., Ltd. (Chengdu, China). The HSA (CAS Number: 70024-90-7, with a purity greater or equal to 96%) was purchased through Sigma-Aldrich (St. Louis, MO, USA). The PCA was dissolved into deionized water to prepare a 3 mM stock solution. A storage solution of 10 uM HSA was prepared with a phosphate-buffered saline (PBS, a pH of 7.4). The concentration of HSA was determined by measuring the absorbance value at a λ_{\max} of 280 nm using a molar extinction coefficient of $35700 \text{ M}^{-1} \text{ cm}^{-1}$. All stock solutions were kept away from light at a temperature of 4 °C.

Methods

Fluorescence spectroscopy measurements

The steady state fluorescence spectroscopy analysis concerning the interaction of PCA with HSA at a temperature of 298 K, 304 K, and 310 K was conducted using a Hitachi F-2500 type Fluorescence Spectrophotometer (Hitachi High-Technologies Co., Ltd., Tokyo, Japan) under the conditions of both excitation and an emission slit width of 5 nm, with an excitation wavelength of 280 nm. A fluorescence signal under the range of a 220 to 500 nm emission wavelength was recorded for all measurements. The photomultiplier tube (PMT) voltage was set to 400 V, and the scanning speed was set to $1500 \text{ nm}\cdot\text{min}^{-1}$. In this study, the fluorescence inner filtering effect was considered, and the intensity of the fluorescence was corrected by the correction formula shown in Eq. 1,

$$F_{cor} = F_{obs} \times e^{(A_{ex}+A_{em})/2} \quad (1)$$

where F_{cor} (arbitrary units, a.u.) and F_{obs} (arbitrary units, a.u.) are the corrected and observed fluorescence intensity, respectively, and A_{ex} (arbitrary units, a.u.) and A_{em} (arbitrary units, a.u.) are the absorbance of PCA at the excitation and emission wavelengths, respectively (Dong *et al.* 2013; Zhu *et al.* 2015).

Ultraviolet-visible absorption (UV-vis) spectroscopy measurements

The UV-vis absorption spectral data were acquired using a UV-2700 type spectrophotometer (Shimadzu Co., Kyoto, Japan) with quartz cuvettes with a 1 cm path length at a temperature of 298 K. The absorption signal was recorded in this experiment at a wavelength range of 190 nm to 500 nm.

Synchronous fluorescence spectroscopy measurements

At a temperature of 298 K, the synchronous fluorescence spectra experiment was performed within a wavelength range of 200 to 400 nm by setting the interval ($\Delta\lambda = \lambda_{em} - \lambda_{ex}$) of the excitation wavelength (λ_{ex}) with the emission wavelength (λ_{em}) at 15 nm and 60 nm, respectively.

Fourier transform infrared spectroscopy measurements

The FT-IR spectra of HSA in the presence and absence of PCA were conducted using a Nicolet 5DX-Fourier transform infrared spectrophotometer (Thermo Electron Corporation, Madison, WI) at a wavenumber range of 4500 to 500 cm^{-1} over 100 scans at a temperature of 298 K.

Molecular docking analysis

Molecular docking uses the 3D structures of two molecules, the ligand and the target, to predict the preferred orientation of the first with respect to the second when bound to each other to form a stable complex (Crampon *et al.* 2022). This is a computational method, which is usually applied to investigate the binding interaction of receptors with ligands (Dong *et al.* 2013). To visualize the binding site and interaction mode of PCA on HSA from the theoretical level, a molecular docking study was conducted by making use of the AutoDock Vina program package (version, Scripps Research, San Diego, CA).

The structure of PCA was drawn using ChemBioDraw Ultra 17.0 (PerkinElmer, Waltham, MA), and was then transformed it into a three-dimensional structure. The MMFF94 force field was used to optimize it. The crystal structure of HSA (PDB ID: 4Z69) was downloaded from the RCSB Protein Data Bank (<http://www.rcsb.org>) (Zhang *et al.* 2015). Before docking, all the water molecules of HSA were deleted, and Gasteiger charges and hydrogen atoms were added, respectively. A grid size of 50 Å, 50 Å, and 50 Å for the X, Y and Z axes was set and the grid center was set at -5.589, 10.425, and 4.433 to cover all possible binding sites. Docking results with the highest score were visualized *via* PyMol software (version, Schrödinger, Inc., New York, NY).

RESULTS AND DISCUSSION

Fluorescence Quenching Study

With the excitation wavelength set to 280 nm, the fluorescence emission spectrum of HSA, in the presence of various concentrations of PCA at a temperature of 298 K, are shown in Fig. 2. The experimental results indicated that HSA had a strong fluorescence emission peak at 337 nm. As the concentration of PCA increased, the intensity of the fluorescence emission peak gradually decreased, suggesting that PCA could interact with HSA to quench the endogenous fluorescence of HSA (Nasruddin *et al.* 2016). Song *et al.* (2012) studied the interaction between phillygenin and HSA, also demonstrating that phillygenin could interact with HSA to quench the endogenous fluorescence of HSA.

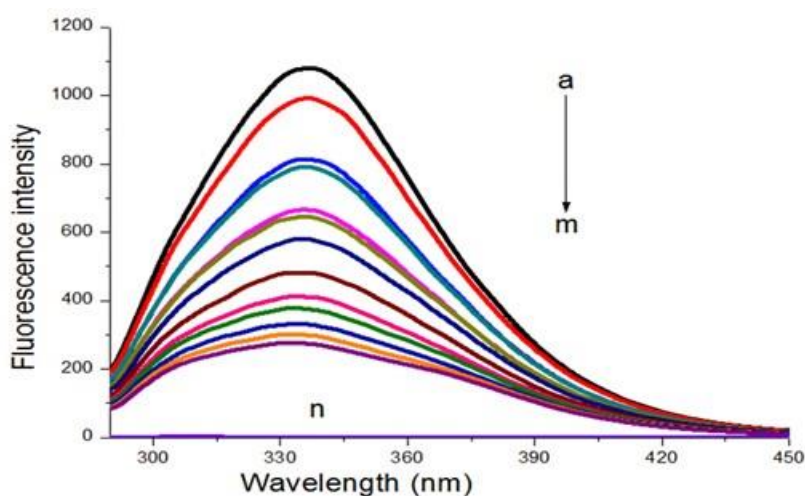


Fig. 2. Fluorescence spectra of HSA (10 μM) without and with PCA (a to m) at a temperature of 298 K, 304 K and 310 K (Note: the concentrations of PCA ranged from 0 μM to 60 μM with a concentration gradient of 5 μM ; and (n) represents the fluorescence spectra of 10 μM of PCA only)

Fluorescence quenching arises due to the molecular interaction between the quencher and the fluorophore. During the quenching process of the fluorophore by the quencher, there are two different quenching mechanisms. One is called a dynamic quenching mechanism, and the other is regarded as a static quenching mechanism. These two quenching mechanisms can be differentiated *via* their different dependence on temperature (Liu *et al.* 2019). For a dynamic quenching mechanism, as the temperature increases, the quenching constant increases, whereas a static quenching mechanism will lead to a new ground-state complex formation between the fluorophore and the quencher (Li *et al.* 2017). In order to obtain the quenching mechanism of HSA by PCA, the fluorescence titration experiment data was analyzed using the Stern-Volmer equation, as shown in Eq. 2,

$$\frac{F_0}{F} = 1 + K_{SV}[Q] = 1 + K_q\tau_0[Q] \quad (2)$$

where F_0 (arbitrary units, a.u.) and F (arbitrary units, a.u.) denote the fluorescence intensities of HSA without and with PCA, respectively, $[Q]$ (mol/L) represents the concentration of PCA, K_{SV} ($L \cdot mol^{-1}$) represents the Stern-Volmer quenching constant, K_q ($L \cdot mol^{-1} \cdot s^{-1}$) is the fluorescence quenching rate constant, and τ_0 (s) is the average lifetime of HSA in the absence of PCA, which is approximately equal to 5.78×10^{-9} s (Zhang and Ma 2013; Morales-Toyo *et al.* 2019).

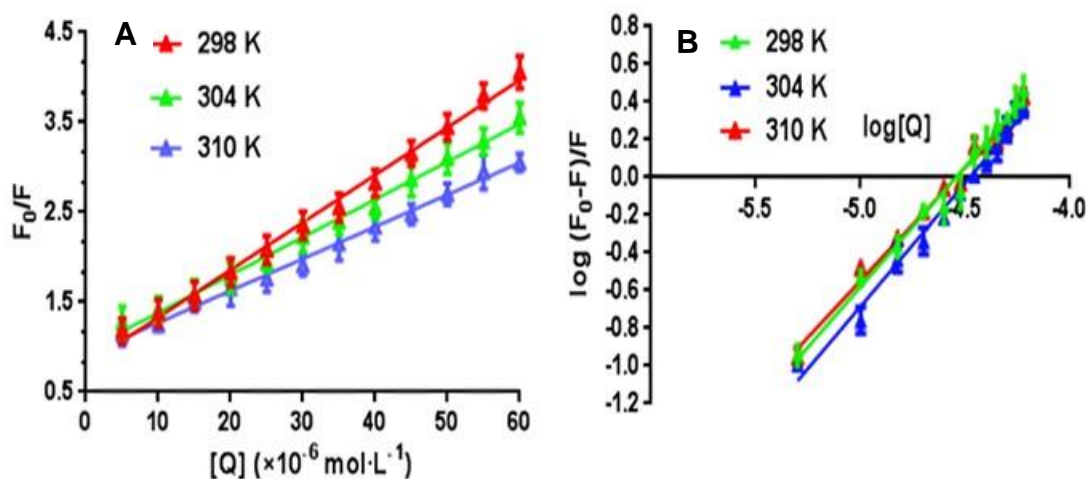


Fig. 3. (A) Stern-Volmer plots of HSA quenched by PCA at a temperature of 298 K, 304 K, and 310 K; and (B) the double logarithmic plots of $\log[(F_0-F)/F]$ against $\log[Q]$ of the fluorescence quenching of HSA by PCA at three different temperatures

The values of K_{SV} at three different temperatures were computed by utilizing the plots of F_0/F against the concentration of PCA $[Q]$, as shown in Fig. 3A. In addition, the values of K_q were calculated utilizing Eq. 2. The related results showed that K_{SV} decreased as the temperature increased and that all values of K_q were higher than the maximum scatter collision quenching constant ($2.0 \times 10^{10} M^{-1} s^{-1}$), as presented in Table 1. This indicated that the quenching mechanism of HSA by PCA was static (Rahman *et al.* 2018). This mechanism could potentially cause the formation of a new ground-state complex of PCA-HSA (Madrakian *et al.* 2014).

Table 1. Stern-Volmer Quenching Constants of HSA by PCA and Binding Parameters at Three Different Temperatures

Temperature (K)	$K_{SV} \times 10^4$ (M^{-1})	$K_q \times 10^{12}$ ($M^{-1} s^{-1}$)	R^2	$K_b \times 10^5$ (M^{-1})	n	R^2
298	5.27 ± 0.06	9.12 ± 0.09	0.9945	4.96 ± 0.13	1.26 ± 0.03	0.9953
304	4.22 ± 0.08	7.30 ± 0.11	0.9975	2.66 ± 0.11	1.21 ± 0.02	0.9908
310	3.53 ± 0.09	6.11 ± 0.14	0.9957	1.22 ± 0.12	1.12 ± 0.04	0.9821

The number of binding sites and binding constants

In the static quenching process of HSA by PCA, the number of binding sites (n , the molar ratio of binding between HSA and PCA) and the binding constants (K_b) of PCA on HSA can be calculated *via* the modified Stern-Volmer equation, as shown in Eq. 3,

$$\log \frac{F_0 - F}{F} = \log K_b + n \log [Q] \quad (3)$$

where F_0 and F denote the fluorescence intensities of HSA without and with PCA, respectively, and $[Q]$ represents the concentration of PCA (Ali *et al.* 2017).

As presented in Fig. 3B, the plots of $\log[(F_0 - F)/F]$ against $\log[Q]$ could be used to obtain the values of n and $\log K_b$. It was deduced from Table 1 that the binding of PCA on HSA had only a binding site with higher affinity (a magnitude of $10^5 M^{-1}$) (Rezende *et al.* 2020). These results suggested that PCA may be slowly metabolized from the body to provide lasting therapeutic effects (Cao *et al.* 2018). In addition, the binding constant of PCA with HSA decreased as the temperature increased. This was consistent with K_{sv} 's dependence on temperature, which suggested that the quenching mechanism was static (Liang *et al.* 2020).

Thermodynamic parameters and interaction forces

The binding interaction of a biomacromolecule with a small ligand can be driven *via* weak forces, *e.g.*, hydrophobic interaction, van der Waals force, electrostatic force, and hydrogen bonding (Khalili and Dehghan 2019). For the binding process of PCA with HSA, the interaction enthalpy change could be treated as a constant when the changes of temperature were not too large (Zhang *et al.* 2015). The values of the enthalpy change (ΔH), entropy change (ΔS), and Gibbs free energy change (ΔG) could be computed using Eqs. 4 and 5,

$$\ln K_b = -\frac{\Delta H}{RT} + \frac{\Delta S}{R} \quad (4)$$

$$\Delta G = -RT \ln K_n \quad (5)$$

where R is the gas constant, which is equal to $8.3145 J mol^{-1} K^{-1}$, T represents the experimental temperature, and K_b is the binding constant (Feroz *et al.* 2015; Ali *et al.* 2018).

The values of the thermodynamic parameters were obtained from the slope and the intercept of the Van't Hoff plot (as shown in Fig. 4) and calculated by Eqs. 4 and 5. As shown in Table 2, the values of ΔG were negative, which suggested that the binding interaction between PCA and HSA was a spontaneous reaction (Tantimongcolwat *et al.* 2019). In addition, the values of both ΔH and ΔS were negative. According to the summary of Ross and Subramanian concerning thermodynamic law, the primary binding interaction forces of a small ligand with a biomacromolecule can be judged. When ΔH is less than 0

and ΔS is less than 0, this suggests that the hydrogen bonding and the van der Waals force are dominant. When ΔH is greater than 0 and ΔS is greater than 0, it indicates the hydrophobic interaction is leading. A ΔH value of approximately 0 and ΔS greater than 0 implies that the electrostatic interaction is dominant. Therefore, it could be concluded that the binding interaction process of PCA with HSA was primarily driven by hydrogen bonding and van der Waals forces, and the result was different from the driving forces of electrostatic and hydrophobic interaction at a low concentration of PCA (Dorraji *et al.* 2014; Wang *et al.* 2018).

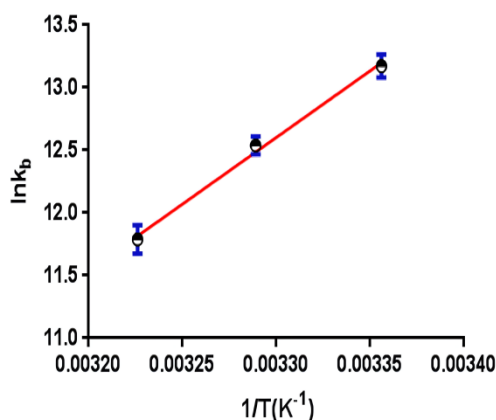


Fig. 4. Van't Hoff plot of HSA quenched by PCA at three different temperatures

Table 2. Thermodynamic Parameters for the Interaction of PCA with HSA at Three Different Temperatures

Temperature (K)	ΔH (kJ mol ⁻¹)	ΔG (kJ mol ⁻¹)	ΔS (J mol ⁻¹ K ⁻¹)
298	-89.53 ± 1.32	-32.56 ± 1.43	-191.18 ± 1.21
304	-	-31.41 ± 1.61	-
310	-	-30.26 ± 1.25	-

Binding distance and non-radiative energy transfer

The possibility of non-radiative energy transfer between HSA and PCA may occur because PCA could quench the intrinsic fluorescence of HSA when the binding interaction of PCA with HSA occurs (Alsaif *et al.* 2020). Therefore, the fluorescence spectra of HSA and the same concentration of the UV-vis absorption spectra of PCA at a wavelength range of 300 to 500 nm at a temperature of 298 K overlapped, which could be used to obtain the energy transfer efficiency (E) between HSA and PCA by using Eq. 6,

$$E = 1 - \frac{F}{F_0} = \frac{R_0^6}{R_0^6 + r^6} \quad (6)$$

where F and F_0 denote the fluorescence intensities of HSA with and without PCA, respectively, r is the binding distance between PCA and HAS, and R_0 is the critical distance at which 50% of the energy gets transferred, which can be computed according to Eq. 7,

$$R_0^6 = 8.79 \times 10^{-25} \cdot k^2 \cdot N^{-4} \cdot \Phi \cdot J(\lambda) \quad (7)$$

where k^2 is the spatial orientation factor of the dipole, which is equal to $2/3^{\text{rds}}$, and N is the average refractive index of medium (1.336 for HSA), Φ is the fluorescence quantum yield

of HSA ($\Phi = 0.118$), and $J(\lambda)$ is the spectra overlap integral between the fluorescence emission spectra of HSA and the absorbance spectra of PCA at a 1 to 1 molar ratio, which can be computed according to Eq. 8,

$$J(\lambda) = \frac{\sum F(\lambda)\varepsilon(\lambda)\lambda^4\Delta\lambda}{\sum F(\lambda)\Delta\lambda} \quad (8)$$

where $\varepsilon(\lambda)$ denotes the molar absorption coefficient of 3,4-dihydroxybenzaldehyde when the wavelength is λ , and $F(\lambda)$ represents the fluorescence intensity of HSA when the wavelength is λ (Sinisi *et al.* 2015; Wang *et al.* 2018; Patil *et al.* 2019).

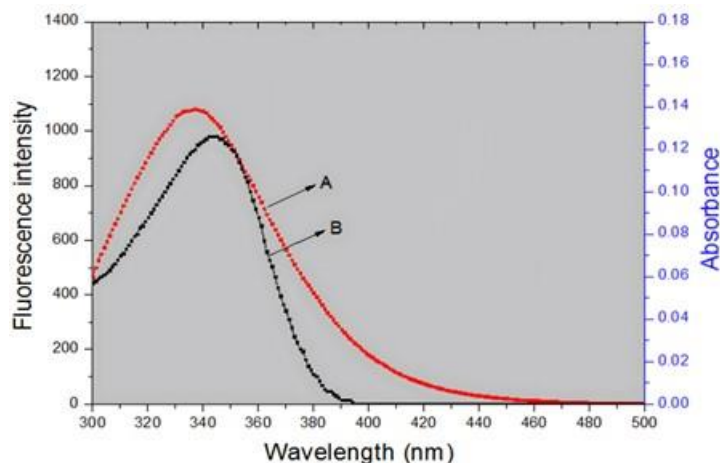


Fig. 5. The overlaps of fluorescence spectra of HAS (A); and the UV-vis absorbance spectra of PCA (B) (Note: the molar ratio of HSA and PCA was 1 to 1 and the concentration of HSA was 10 μ M)

The overlaps of the absorbance spectrum of free PCA with the fluorescence emission spectrum of free HSA are presented in Fig. 5. The values of E , R_0 , r , and $J(\lambda)$ were calculated by using Eq. 6 through 8, and the related results are shown in Table 3. It could be seen that r was less than 8 nm as well as the fact that $0.5R_0$ was less than r , which was less than $1.5R_0$, which suggested that the energy transfer between HSA and PCA may happen with a high probability (More *et al.* 2011).

Table 3. Förster Resonance Energy Transfer Parameters between HSA and PCA

$J \times 10^{-14}$ ($\text{cm}^3 \text{M}^{-1}$)	E	R_0 (nm)	R (nm)
8.25	0.19	3.47	4.42

Ultraviolet-visible absorption (UV-vis) absorption spectroscopy study

Ultraviolet-visible absorption spectroscopy is an effective method that can be used to confirm the structural changes of a protein and verify the complex formation when the binding interaction of a protein and drug occurs (Siddiqi *et al.* 2018). The aromatic amino acid residues, including tryptophan, tyrosine, and phenylalanine, are responsible for an obvious absorbance peak at approximately 280 nm, which is due to the $\pi \rightarrow \pi^*$ transition of the phenyl rings in these residues (Kazemi *et al.* 2016). As shown in Fig. 6A, the absorbance peak intensity of HSA at approximately 280 nm was enhanced at increased concentrations of PCA, which suggested that a new complex of PCA-HSA was formed with a molar ratio of 1:1, which was mainly driven by hydrogen bonding and van der Waals

forces. This was further shown by the results of the difference in the UV-vis absorption spectrum (Fig. 6B) (Mote *et al.* 2011; Wang *et al.* 2020). Furthermore, these results indicated that the fluorescence quenching mechanism of HSA by PCA was static (Morales-Toyo *et al.* 2019).

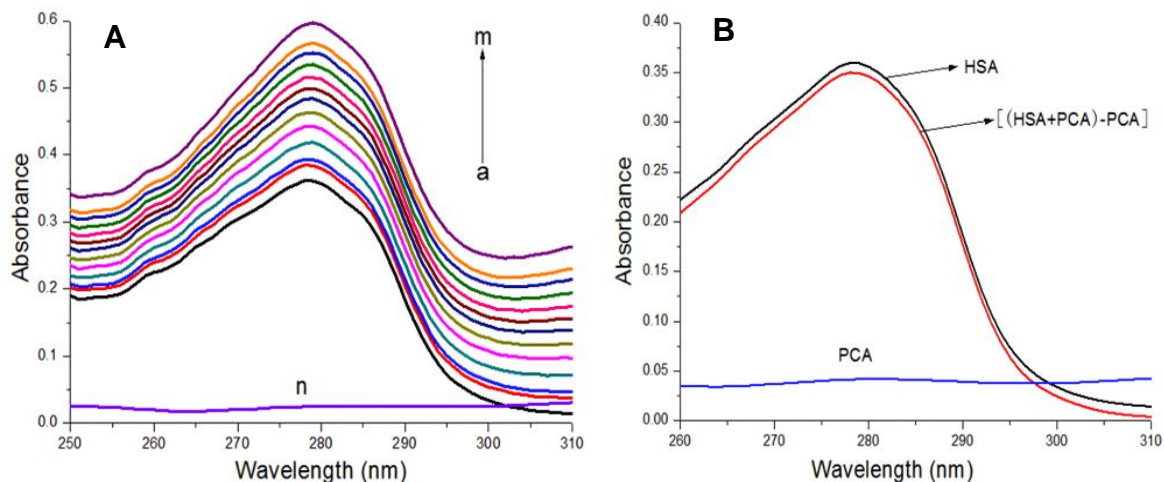


Fig. 6. (A) UV-vis absorption spectra of HSA (10 μM) without and with PCA (a through m) at a temperature of 298 K (Note: the concentrations of PCA were from 0 μM to 60 μM with a concentration gradient of 5 μM and (n) represents the UV-vis absorption spectra of 5 μM PCA only); and (B) the difference in the UV-vis absorption spectra of HSA (10 μM) with PCA (10 μM) at a temperatures of 298 K.

Synchronous fluorescence spectroscopy study

Synchronous fluorescence spectroscopy can be utilized for detecting the changes in the microenvironment around the tryptophan and tyrosine residues on HAS (Al-Shabib *et al.* 2017). In this experiment, the values of the interval ($\Delta\lambda$) of excitation wavelength with emission wavelength were set to 15 and 60 nm, respectively (Chi *et al.* 2018). The synchronous fluorescence spectra of HSA with different concentrations of PCA were measured (Fig. 7).

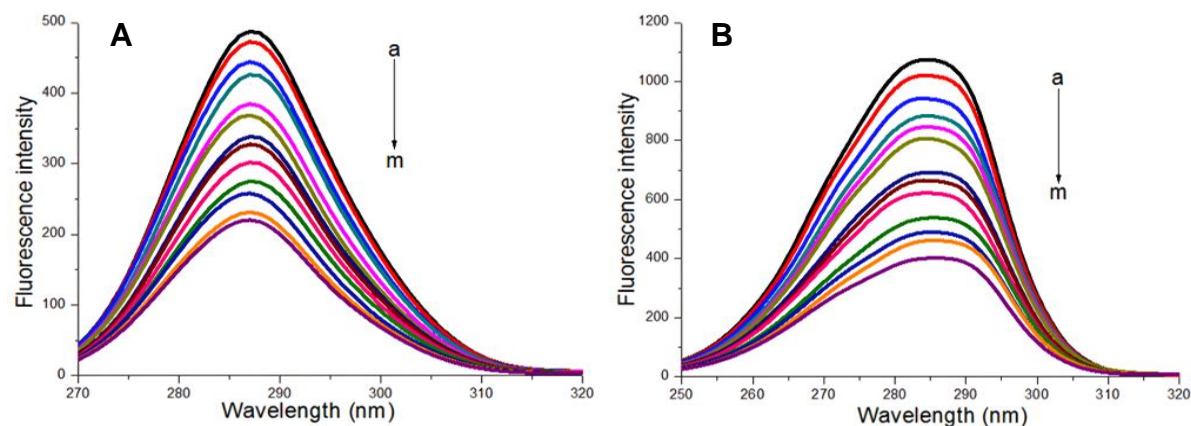


Fig. 7. Synchronous fluorescence spectra of HSA (10 μM) without and with PCA (a through m) at a temperature of 298 K: (A) $\Delta\lambda = 15$ nm; and (B) $\Delta\lambda = 60$ nm (Note: the concentrations of PCA were from 0 to 60 μM with a concentration gradient of 5 μM)

It could be observed that at two different $\Delta\lambda$, the synchronous fluorescence intensity of HSA was markedly reduced as the concentration of PCA increased. Moreover, the maximum wavelength of the emission peak of tryptophan appeared in the red shift and no considerable shift change was found in the maximum wavelength of the emission peak of tyrosine. This suggests that the polarity of the microenvironment around tryptophan increased, whereas the polarity of the microenvironment around tyrosine hardly changed (Dong *et al.* 2019).

Fourier-transform infrared (FT-IR) spectroscopy study

Fourier-transform infrared spectroscopy is a sound method that can be used to explore the changes in the secondary structure of a protein. The IR spectra of a protein can exhibit some special amide bands, known as amide I and amide II, which denote different vibrations of the peptide moiety (Yang *et al.* 2011). Among these amide bands, the amide I band in the region 1600 to 1700 cm^{-1} is primarily due to C=O stretching, whereas the amide II band (approximately 1548 cm^{-1}) is primarily due to C-N stretching and N-H bending. As shown in Fig. 8, it was observed that the wavenumber of the amide I band shifted from 1643 to 1639 cm^{-1} . In addition, the wavenumber of the amide II band shifted from 1542 to 1541 cm^{-1} . These results suggested that PCA changed the secondary structure of HSA, thereby causing its conformational changes (Khalili and Dehghan 2019).

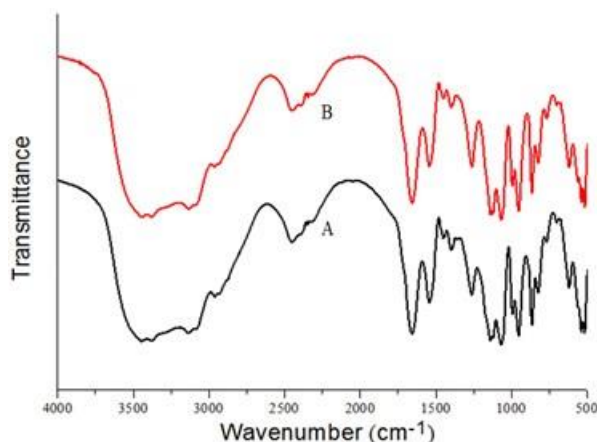


Fig. 8. FT-IR spectra of HSA without and with PCA at a temperature of 298 K: (A) the FT-IR spectra of 10 μM HSA only; and (B) the FT-IR spectra of HSA (10 μM) in the presence of PCA (10 μM)

Molecular docking results

The binding free energy (-6.0 kJ mol^{-1}) with the highest score was used as the optimal result. The energy difference between the molecular docking and the thermodynamic analysis may be because the docking analysis was conducted under simulation of a vacuum environment, thus neglecting the desolvation energy. Furthermore, the X-ray structure of HSA may be different from X-ray structure in the aqueous system (Wang *et al.* 2014). It could be seen that PCA was located in subdomain IB (Fig. 9A). As shown in Fig. 9B, PCA can form hydrogen bonding interactions with Tyr-161, Leu-185, and Ser-193. In addition, hydrophobic interaction occurred between PCA and Ile-142, Phe-149, Leu-154, Phe-157, Tyr-161, and Leu-185 (Fig. 10). The combined results of the thermodynamic parameters and molecular docking analysis implied that the interaction forces of PCA with HSA included hydrogen bonding, van der Waals forces, and hydrophobic interaction.

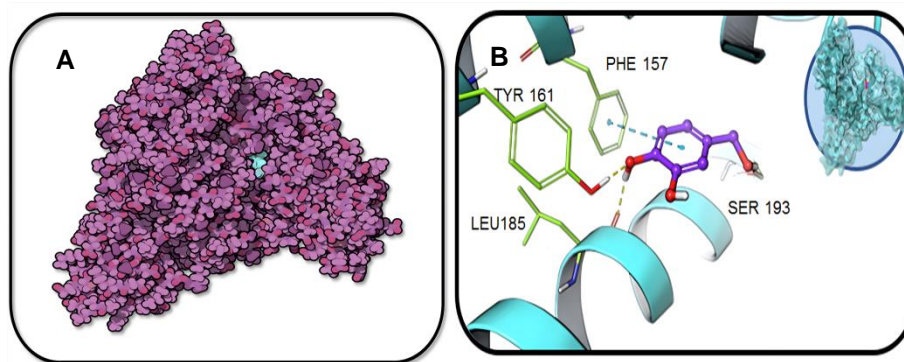


Fig. 9. Docking results between the HSA and PCA with the highest score. The PCA was located in subdomain IB and interacted with some amino acid residues *via* hydrogen bonding

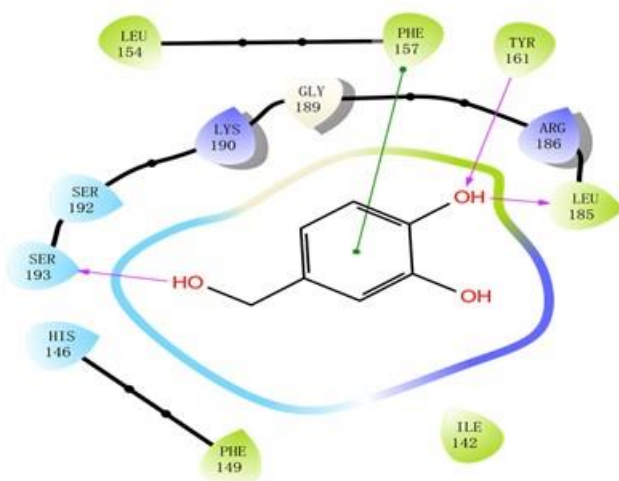


Fig. 10. PCA interacted with some amino acid residues of HSA *via* hydrogen bonding and hydrophobic interaction

CONCLUSIONS

1. In this work, multiple spectroscopic analysis, including fluorescence, synchronous fluorescence, UV-vis, FT-IR spectroscopy, and the molecular docking method, were utilized to study the binding interaction of protocatechualdehyde (PCA) with human serum albumin (HSA) *in vitro*. The results suggested that PCA quenched the intrinsic fluorescence of HSA *via* a static mechanism.
2. The binding affinity between PCA and HSA was strong. The binding of both was driven primarily by hydrogen bonding and the Van der Waals force at a high concentration of PCA. The binding distance was 4.42 nm and the binding site for PCA on the HSA molecule was located in subdomain IB.
3. In addition, PCA induced microenvironmental and secondary structural changes of HSA. This work may provide reference for studying the binding properties of PCA with HSA *in vivo*.

ACKNOWLEDGMENTS

The authors are grateful for the support of the National Natural Science Foundation of Henan (Grant No. 212300410228), the Scientific and Technological Planning in Henan Province (Grant No. 212102110314), Youth Foundation of Xinyang Agriculture and Forestry University (Grant No. QN2021030), Youth Foundation of Xinyang Agriculture and Forestry University (Grant No. 2019LG002), and Youth Foundation of Xinyang Agriculture and Forestry University (Grant No. 2019LG009).

REFERENCES CITED

- Ali, M. S., and Al-Lohedan, H. A. (2017). "Deciphering the interaction of procaine with bovine serum albumin and elucidation of binding site: A multi spectroscopic and molecular docking study," *Journal of Molecular Liquids* 236, 232-240. DOI: 10.1016/j.molliq.2017.04.020
- Ali, M. S., and Al-Lohedan, H. A. (2018). "Spectroscopic and computational evaluation on the binding of safranal with human serum albumin: Role of inner filter effect in fluorescence spectral correction," *Spectrochimica Acta Part A: Molecular and Biomolecular Spectroscopy* 203, 434-442. DOI: 10.1016/j.saa.2018.05.102
- Almutairi, F. M., Ajmal, M. R., Siddiqi, M. K., Amir, M., and Khan, H. R. (2020). "Multi-spectroscopic and molecular docking technique study of the azelastine interaction with human serum albumin," *Journal of Molecular Structure* 1201, 1-7. DOI: 10.1016/j.molstruc.2019.127147
- Alsaif, N. A., Wani, T. A., Bakheit, A. H., and Zargar, S. (2020). "Multi-spectroscopic investigation, molecular docking and molecular dynamic simulation of competitive interactions between flavonoids (quercetin and rutin) and sorafenib for binding to human serum albumin," *International Journal of Biological Macromolecules* 165, 2451-2461. DOI: 10.1016/j.ijbiomac.2020.10.098
- Al-Shabib, N. A., Khan, J. M., Ali, M. S., Al-Lohedan, H. A., Khan, M. S., Al-Senaigy, A. M., Husain, F. M., and Shamsi, M. B. (2017). "Exploring the mode of binding between food additive "butylated hydroxytoluene (BHT)" and human serum albumin: Spectroscopic as well as molecular docking study," *Journal of Molecular Liquids* 230, 557-564. DOI: 10.1016/j.molliq.2017.01.066
- Cao, X., He, Y., Liu, D., He, Y., Hou, X., Cheng, Y., and Liu, J. (2018). "Characterization of interaction between scoparone and bovine serum albumin: Spectroscopic and molecular docking methods," *RSC Advances* 8(45), 25519-25525. DOI: 10.1039/C8RA04065F
- Caruso, I. P., Filho, J. M. B., Araújo, A. S., Souza, F. P. d., Fossey, M. A., and Cornélio, M. L. (2016). "An integrated approach with experimental and computational tools outlining the cooperative binding between 2-phenylchromone and human serum albumin," *Food Chemistry* 196, 935-942. DOI: 10.1016/j.foodchem.2015.10.027
- Chi, Q., Li, Z., Huang, J., Ma, J., and Wang, X. (2018). "Interactions of perfluorooctanoic acid and perfluorooctanesulfonic acid with serum albumins by native mass spectrometry, fluorescence and molecular docking," *Chemosphere* 198, 442-449. DOI: 10.1016/j.chemosphere.2018.01.152
- Crampon, K., Giorkallos, A., Deldossi, M., Baud, S., and Steffanel, L. A. (2022). "Machine-learning methods for ligand-protein molecular docking," *Drug discovery*

- today 27(1), 151-164. DOI: 10.1016/j.drudis.2021.09.007
- Cui, F., Zhang, Q., Yan, Y., Yao, X., Qu, G., and Lu, Y. (2008). "Study of characterization and application on the binding between 5-iodouridine with HSA by spectroscopic and modeling," *Carbohydrate Polymers* 73(3), 464-472. DOI: 10.1016/j.carbpol.2007.12.032
- Dong, C., Ma, S., and Liu, Y. (2013). "Studies of the interaction between demeclocycline and human serum albumin by multi-spectroscopic and molecular docking methods," *Spectrochimica Acta Part A: Molecular and Biomolecular Spectroscopy* 103, 179-186. DOI: 10.1016/j.saa.2012.10.050
- Dong, Q., Yu, C., Li, L., Nie, L., Zhang, H., and Zang, H. (2019). "Analysis of hydration water around human serum albumin using near-infrared spectroscopy," *International Journal of Biological Macromolecules* 138, 927-932. DOI: 10.1016/j.ijbiomac.2019.07.183
- Dorraj, M. S. S., Azar, V. P., and Rasoulifard, M. H. (2014). "Interaction between deferiprone and human serum albumin: Multi-spectroscopic, electrochemical and molecular docking methods," *European Journal of Pharmaceutical Sciences* 64, 9-17. DOI: 10.1016/j.ejps.2014.08.001
- Duan, L., Xiang, H., Yang, X., Liu, L., Tian, Z., Tian, H., and Li, J. (2019). "The influences of 3,4-dihydroxybenzaldehyde on the microstructure and stability of collagen fibrils," *Polymer Degradation and Stability* 161, 198-205. DOI: 10.1016/j.polymdegradstab.2019.01.031
- Feroz, S. R., Mohamad, S. B., Lee, G. S., Malek, S. N. A., and Tayyab, S. (2015). "Supra molecular interaction of 6-shogaol, a therapeutic agent of *Zingiber officinale* with human serum albumin as elucidated by spectroscopic, calorimetric and molecular docking methods," *Phytomedicine* 22(6), 621-630. DOI: 10.1016/j.phymed.2015.03.016
- Guo, J., He, Z., Wu, S., Zeng, M., and Chen, J. (2020). "Effects of concentration of flavor compounds on interaction between soy protein isolate and flavor compounds," *Food Hydrocolloids* 100, article no. 105388. DOI: 10.1016/j.foodhyd.2019.105388
- Kazemi, Z., Rudbari, H. A., Sahihi, M., Mirkhani, V., Moghadam, M., Tangestaninejad, S., Mohammadpoor-Baltork, I., and Gharaghani, S. (2016). "Synthesis, characterization and biological application of four novel metal-Schiff base complexes derived from allylamine and their interactions with human serum albumin: Experimental, molecular docking and ONIOM computational study," *Journal of Photochemistry and Photobiology B: Biology* 162, 448-462. DOI: 10.1016/j.jphotobiol.2016.07.003
- Khalili, L., and Dehghan, G. (2019). "A comparative spectroscopic, surface plasmon resonance, atomic force microscopy and molecular docking studies on the interaction of plant derived conferone with serum albumins," *Journal of Luminescence* 211, 193-202. DOI: 10.1016/j.jlumin.2019.03.048
- Li, G., Huang, J., Chen, T., Wang, X., Zhang, H., and Chen, Q. (2017). "Insight into the interaction between chitosan and bovine serum albumin," *Carbohydrate Polymers* 176, 75-82. DOI: 10.1016/j.carbpol.2017.08.068
- Li, H., Li K., Liu, H., Jing, T., Song X., Xue L., Li C., and Shen W. (2016). "The effect of VOCs from the branches and leaves of *Pistacia chinensis* Bunge and *Juniperus chinensis* cv. Kaizuka on mouse behavior," *BioResources* 11(4), 10226-10239. DOI: 10.15376/biores.11.4.10226-10239
- Li, X., Xiang, B., Shen, T., Xiao, C., Dai, R., He, F., and Lin, Q. (2020). "Anti-

- neuroinflammatory effect of 3,4-dihydroxybenzaldehyde in ischemic stroke,” *International Immunopharmacology* 82, 1-11. DOI: 10.1016/j.intimp.2020.106353
- Liang, C.-Y., Pan, J., Bai, A.-M., and Hu, Y.-J. (2020). “Insights into the interaction of human serum albumin and carbon dots: Hydrothermal synthesis and biophysical study,” *International Journal of Biological Macromolecules* 149, 1118-1129. DOI: 10.1016/j.ijbiomac.2020.01.238
- Liu, F., Zhang, Y., Yu, Q., Shen, Y., Zheng, Z., Cheng, J., Zhang, W., and Ye, Y. (2019). “Exploration of the binding between ellagic acid, a potentially risky food additive, and bovine serum albumin,” *Food and Chemical Toxicology* 134, 1-7. DOI: 10.1016/j.fct.2019.110867
- Madrakian, T., Bagheri, H., Afkhami, A., and Soleimani, M. (2014). “Spectroscopic and molecular docking techniques study of the interaction between oxymetholone and human serum albumin,” *Journal of Luminescence* 155, 218-225. DOI: 10.1016/j.jlumin.2014.06.047
- Malhotra, S., and Karanicolas, J. (2017). “When does chemical elaboration induce a ligand to change its binding mode?,” *Journal of Medicinal Chemistry* 60(1), 128-145. DOI: 10.1021/acs.jmedchem.6b00725
- Morales-Toyo, M., Glidewell, C., Bruno-Colmenares, J., Cubillán, N., Sánchez-Colls, R., Alvarado, Y., and Restrepo, J. (2019). “Synthesis of (E)-Ethyl-4-(2-(furan-2-ylmethylene)hydrazinyl)benzoate, crystal structure, and studies of its interactions with human serum albumin by spectroscopic fluorescence and molecular docking methods,” *Spectrochimica Acta Part A: Molecular and Biomolecular Spectroscopy* 216, 375-384. DOI: 10.1016/j.saa.2019.03.028
- More, V. R., Anbhule, P. V., Lee, S. H., Patil, S. R., and Kolekar, G. B. (2011). “Fluorimetric study on the interaction between norfloxacin and proflavine hemisulphate,” *Journal of Fluorescence* 21, 1789-1796. DOI: 10.1007/s10895-011-0873-8
- Mote, U. S., Patil, S. R., Bhosale, S. H., Han, S. H., and Kolekar, G. B. (2011). “Fluorescence resonance energy transfer from tryptophan to folic acid in micellar media and deionised water,” *Journal of Photochemistry and Photobiology B: Biology* 103(1), 16-21. DOI: 10.1016/j.jphotobiol.2011.01.006
- Nasruddin, A. N., Feroz, S. R., Mukarram, A. K., Mohamad, S. B., and Tayyab, S. (2016). “Fluorometric and molecular docking investigation on the binding characteristics of SB202190 to human serum albumin,” *Journal of Luminescence* 74, 77-84. DOI: 10.1016/j.jlumin.2016.02.004
- Ni, Y., Zhu, R., and Kokot, S. (2011). “Competitive binding of small molecules with biopolymers: a fluorescence spectroscopy and chemometrics study of the interaction of aspirin and ibuprofen with BSA,” *Analyst* 136(22), 4794-4801. DOI: 10.1039/c1an15550d
- Nusrat, S., Masroor, A., Zaman, M., Siddiqi, M. K., Ajmal, M. R., Zaidi, N., Abdelhameed, A. S., and Khan, R. H. (2018). “Interaction of catecholamine precursor L-Dopa with lysozyme: A biophysical insight,” *International Journal of Biological Macromolecules* 109, 1132-1139. DOI: 10.1016/j.ijbiomac.2017.11.107
- Patil, S. R., Salunkhe, S. M., Wakshe, S. B., Karnik, K. S., Sarkate, A. P., Patrawale, A. A., Anbhule, P. V., and Kolekar, G. B. (2019). “Spectral elucidation with molecular docking study between isatin analogous and bovine serum albumin,” *Chemical Data Collections* 22, 1-11. DOI: 10.1016/j.cdc.2019.100254
- Rahman, Y., Afrin, S., and Tabish, M. (2018). “Interaction of pirenzepine with bovine

- serum albumin and effect of β -cyclodextrin on binding: A biophysical and molecular docking approach,” *Archives of Biochemistry and Biophysics* 652, 27-37. DOI: 10.1016/j.abb.2018.06.005
- Rezende, J. P. d., Hudson, E. A., Paula, H. M. C. D., Meinel, R. S., Silva, A. D. D., Silva, L. H. M. D., and Pires, A. C. d. S. (2020). “Human serum albumin-resveratrol complex formation: Effect of the phenolic chemical structure on the kinetic and thermodynamic parameters of the interactions,” *Food Chemistry* 307, 1-8. DOI: 10.1016/j.foodchem.2019.125514
- Siddiqi, M., Nusrat, S., Alam, P., Malik, S., Chaturvedi, S. K., Ajmal, M. R., Abdelhameed, A. S., and Khan, R. H. (2018). “Investigating the site selective binding of busulfan to human serum albumin: Biophysical and molecular docking approaches,” *Journal of Biological Macromolecules* 107(Part B), 1414-1421. DOI: 10.1016/j.ijbiomac.2017.10.006
- Sinisi, V., Forzato, C., Cefarin, N., Navarini, L., and Berti, F. (2015). “Interaction of chlorogenic acids and quinides from coffee with human serum albumin,” *Food Chemistry* 168, 332-340. DOI: 10.1016/j.foodchem.2014.07.080
- Song, W., Ao, M. Z., Shi, Y., Yuan, L. F., Yuan, X. X., and Yu, L. J. (2012). “Interaction between phillygenin and human serum albumin based on spectroscopic and molecular docking,” *Spectrochimica Acta Part A: Molecular and Biomolecular Spectroscopy* 85, 120-126. DOI: 10.1016/j.saa.2011.09.044
- Sun, Q., He, J., Yang, H., Li, S., Zhao, L., and Li, H. (2017). “Analysis of binding properties and interaction of thiabendazole and its metabolite with human serum albumin via multiple spectroscopic methods,” *Food Chemistry* 233, 190-196. DOI: 10.1016/j.foodchem.2017.04.119
- Tantimongcolwat, T., Prachayasittikul, S., and Prachayasittikul, V. (2019). “Unravelling the interaction mechanism between clioquinol and bovine serum albumin by multi-spectroscopic and molecular docking approaches,” *Spectrochimica Acta Part A: Molecular and Biomolecular Spectroscopy* 216, 25-34. DOI: 10.1016/j.saa.2019.03.004
- Tian, J., Chen, C., and Xue, M. (2011). “The interaction between protocatechuic aldehyde and human serum albumin using three-dimensional fluorescence techniques,” *Journal of Spectroscopy* 26, 195-201. DOI: 10.1155/2011/932060
- Wang, Y., Zhang, G., and Wang, L. (2014). “Interaction of prometryn to human serum albumin: Insights from spectroscopic and molecular docking studies,” *Pesticide Biochemistry and Physiology* 108, 66-73. DOI: 10.1016/j.pestbp.2013.12.006
- Wang, X., He, L.-L., Liu, B., Wang, X.-F., Xu, L., and Sun, T. (2018). “Reactive oxygen species generation and human serum albumin damage induced by the combined effects of ultrasonic irradiation and brilliant cresyl blue,” *International Journal of Biological Macromolecules* 120(Part B), 1865-1871. DOI: 10.1016/j.ijbiomac.2018.10.002
- Wang, Y., Liu, J., Zhu, M., Wang, L., Zen, X., Fan, S., Wang, Z., Li, H., Na, R., Zhao, X., *et al.* (2018). “Biophysical characterization of interactions between falcarinol-type polyacetylenes and human serum albumin via multispectroscopy and molecular docking techniques,” *Journal of Luminescence* 200, 111-119. DOI: 10.1016/j.jlumin.2018.03.082
- Wang, L., Dong, J., Li, R., Zhao, P., Kong, J., and Li, L. (2020). “Elucidation of binding mechanism of dibutyl phthalate on bovine serum albumins by spectroscopic analysis and molecular docking method,” *Spectrochimica Acta Part A: Molecular and*

- Biomolecular Spectroscopy* 230, 1-9. DOI: 10.1016/j.saa.2020.118044
- Wang, H., Xia, X., Yin, X., Liu, H., Chem, Q., and Kong, B. (2021). "Investigation of molecular mechanisms of interaction between myofibrillar proteins and 1-heptanol by multiple spectroscopy and molecular docking methods," *International Journal of Biological Macromolecules* 193, 672-680. DOI: 10.1016/j.ijbiomac.2021.10.105
- Yan, J., Wu, D., Ma, X., Wang, L., Xu, K., and Li, H. (2015). "Spectral and molecular modeling studies on the influence of β -cyclodextrin and its derivatives on aripiprazole-human serum albumin binding," *Carbohydrate Polymers* 131, 65-74. DOI: 10.1016/j.carbpol.2015.05.037
- Yang, Q., Zhou, X., and Chen, X. (2011). "Combined molecular docking and multi-spectroscopic investigation on the interaction between Eosin B and human serum albumin," *Journal of Luminescence* 131(4), 581-586. DOI: 10.1016/j.jlumin.2010.10.033
- Yue, Y., Wang, Z., Wang, Z., Zhang, Y., and Liu, J. (2018). "A comparative study of binding properties of different coumarin-based compounds with human serum albumin," *Journal of Molecular Structure* 1169, 75-80. DOI: 10.1016/j.molstruc.2018.05.060
- Zhang, G., and Ma, Y. (2013). "Mechanistic and conformational studies on the interaction of food dye amaranth with human serum albumin by multispectroscopic methods," *Food Chemistry* 136(2), 442-449. DOI: 10.1016/j.foodchem.2012.09.026
- Zhang, X., Gao, R., Li, D., Yin, H., Zhang, J., Cao, H., and Zheng, X. (2015). "Study on interaction between 5-Bromo-4-thio-2-deoxyuridine and human serum albumin by spectroscopy and molecular docking," *Spectrochimica Acta Part A: Molecular and Biomolecular Spectroscopy* 136(Part C), 1775-1781. DOI: 10.1016/j.saa.2014.10.081
- Zhang, Y., Lee, P., Liang, S., Zhou, Z., Wu, X., Yang, F., and Liang, H. (2015). "Structural basis of non-steroidal anti-inflammatory drug diclofenac binding to human serum albumin," *Chemical Biology & Drug Design* 86(5), 1178-1184. DOI: 10.1111/cbdd.12583
- Zhu, G., Wang, Y., Xi, L., Liu, J., Wang, H., and Du, L. (2015). "Spectroscopy and molecular docking studies on the binding of propyl gallate to human serum albumin," *Journal of Luminescence* 159, 188-196. DOI: 10.1016/j.jlumin.2014.11.020

Article submitted: December 2, 2021; Peer review completed: February 12, 2022;
Revised version received: March 3, 2022; Accepted: March 6, 2022; Published: March 25, 2022.

DOI: 10.15376/biores.17.2.2680-2695